Energy Analysis of a Solar-Driven Hybrid Air Conditioning System with an Absorption Heat Pump and a Desiccant Evaporative Cooling System.

Juan Prieto[1], Ruslán Kotegov[1], Francisco Comino[2], José Ignacio Ajona[3], Manuel Ruiz de Adana[2], Alberto Coronas[1]

[1] Universitat Rovira i Virgili, Mechanical Engineering Department, CREVER, Avda. Països Catalans 26, 43007, Tarragona (Spain)

[2] Dto. De Química-Física y Termodinámica Aplicada, Escuela Politécnica Superior, Universidad de Córdoba, Campus de Rabanales, Antigua Carretera Nacional IV, km 396, 14071, Córdoba (Spain)

[3] Seenso Renoval S.L, C. Aravaca 30, 28040, Madrid (Spain)

Abstract

In this paper it is presented a HVAC system with a solar driven single-effect absorption heat pump with condensation heat recovery and an air-handling unit with a desiccant wheel and an evaporative cooler. The integration of both cooling technologies allows to achieve a good overall performance as the desiccant system handles the latent loads and the absorption chiller the sensible loads. Moreover, the desiccant system is activated with the heating provided by the condensation heat from the absorption heat pump, which minimizes the amount of heating that must be provided by a solar concentrator coupling flat sun-tracking mirrors to a fixed tilt evacuated tubular collectors.

The size and the operational conditions of the integrated system are selected in order to optimize the overall performance of the system under different ambient conditions (solar radiation, ambient temperature and ambient humidity ratio). An overall thermal COP of 1.21 is reached in the hybrid system.

Keywords: Type your keywords here, separated by commas, in italic

1. Introduction

In this work, it is presented a solar cooling system with an absorption heat pump (AHP) with condensation heat recovery and an air-handling unit (AHU) with a desiccant wheel (DW), and an indirect evaporative cooler (IEC). The integration of both cooling technologies allows achieving a good overall performance as the desiccant system handles the latent loads and the AHP the sensible loads. Moreover, the desiccant system is activated with the heating provided by the condensation heat from the AHP, which minimizes the amount of heating that must be provided by the solar panels.

Therefore, the main objective is the energy analysis of an integrated solar cooling system comprised of the mentioned technologies when it is implemented in Tarragona, Spain. The expected results are referred to the number of solar panels, the AHP cooling and heating capacity, the AHU cooling capacity at nominal conditions, and the operating conditions that maximizes the overall performance of the system.

2. System description

A hybrid solar cooling system comprised of an AHP with condensation heat recovery and AHU with a desiccant wheel (DW) and an indirect evaporative cooler (IEC) is evaluated. The activation heat required by the AHP is provided by evacuated tube solar collectors (ETC) with low concentrator (<2) in both sides of them. In addition, the released heat in the AHP condenser is used to regenerate the DW. The description of each component of the system and the integration of all of them is presented below.

2.1. Absorption heat pump

The AHP is based on a single-effect absorption H_2O/LiBr chiller with its cycle modified to recover the heat of condensation at a useful temperature level (Juan Prieto et al. 2022). Thereby, the performance of the AHP is improved and enables the delivery of two useful outputs simultaneously. Besides, part of the condensation heat is also used internally for the LiBr solution preheating to reduce the generator heat input. Figure 1 shows a schematic

doi:10.18086/eurosun.2022.06.08 Available at http://proceedings.ises.org

layout of the AHP. As it can be seen in this Figure, two new components are incorporated: a preheater (PH) and a water-solution heat exchanger (WSHE). The weak, in LiBr, solution is preheated before entering to the solution heat exchanger (SHE) by using the heat released during condensation of part of the vapor leaving the generator (stream 7). The PH is implemented in parallel with the condenser (C). The water-solution heat exchanger cools the strong, in LiBr, solution leaving the SHE while producing hot water. Moreover, the heat released by the condenser is at useful temperature level so that it can be also used for heating applications. Thus, the hot water leaving the WSHE and the C is supplied to regenerate the DW of the AHU.

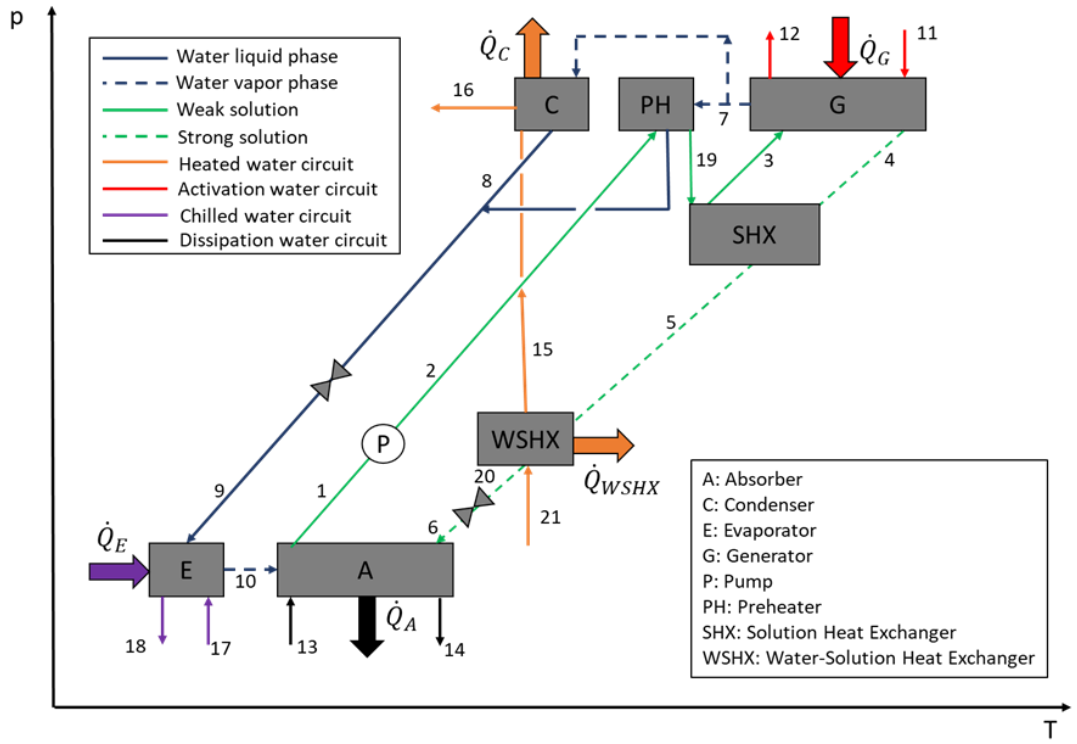

Fig. 1: Single-effect absorption heat pump for simultaneous heating and cooling production (Juan Prieto et al. 2022).

Along with the components of the cycle, the working conditions have also been changed in this system. The Dühring plot for the improved absorption HP with CHR is represented in Figure 2. Red lines illustrate the conditions of the proposed single-effect H_2O/LiBr AHP. Conditions in Figure 2 correspond to the thermodynamic states of the system in Figure 1. As it can be noted, this system also operates at two different pressure levels. The absorber and evaporator operate at a low-pressure level, which is around 1 kPa. The condenser, generator, preheater, solution heat exchanger, and water-solution heat exchanger operate at a high-pressure level of around 15 kPa. In opposition to the conventional cycle, the high pressure is doubled up. The temperature of condensation depends upon the actual pressure, the greater the pressure the greater the condensing temperature. Thus, the elevated pressure permits to make use of condensation heat for a variety of heating applications and for preheating the weak solution as well. Furthermore, due to changes in the operating conditions, a few alterations should be made to enhance the overall efficiency of the absorption cycle.

In this regard, the cycle operates at four temperature levels in place of three (J. Prieto et al., 2022):

- The evaporator produces cooling, and the temperature ranges from 5 to 15 °C;
- The absorber dissipates heat to the ambient because the heat is useless for most applications at these temperature levels. The temperature ranges from 25 to 40 °C;
- The condenser heating (condensation heat) can be used, as the temperature ranges from 50 to 60 °C;
- The generator requires a heat supply, and the temperature ranges from 85 to 120 °C.

As it can be observed, Figure 2 clearly shows that crystallization risk under these conditions is minimal because Point 6 is far from the crystallization line. Consequently, the new cycle operates under more favorable conditions compared to the conventional cycle. In this sense, the generator operating temperatures can be greater

than in the conventional cycle. Besides, the lack of crystallization allows the use of a SHE with higher effectiveness, and, as a result, the total cycle COP is higher. Furthermore, the preheated condition at State 19 before the SHE leads to a higher temperature at State 5. This fact allows the incorporation of the WSHE into the system after the SHE to extract additional heat from the cycle.

Eventually, the differential between the strong and poor solution mass fraction is lower contrasted with the conventional cycle. Consequently, to obtain the equivalent amount of heating and cooling it is imperative to increase the solution mass flow rate, and it implies that a more powerful solution pump must be installed.

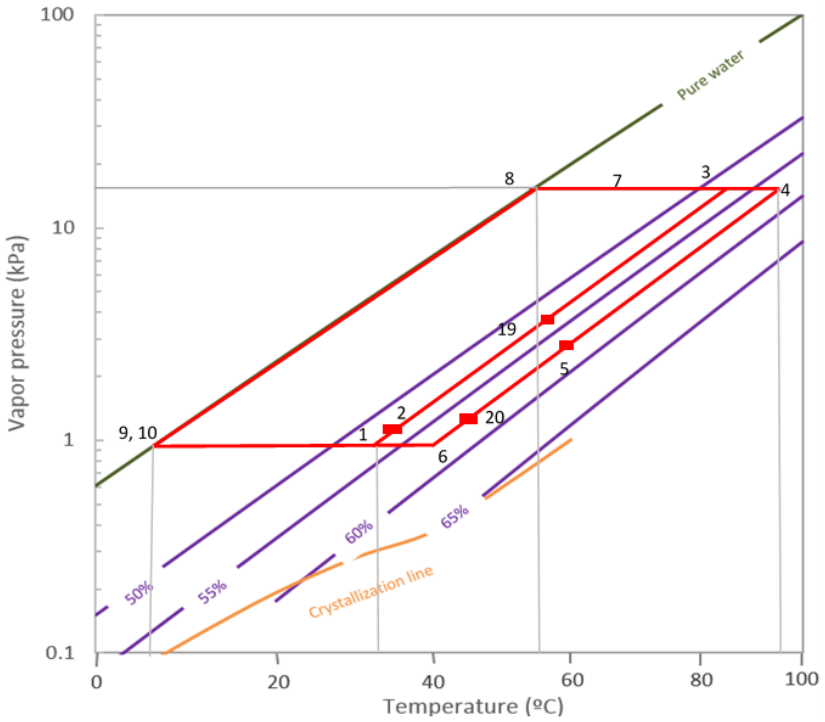

Fig. 2: Dühring plot for the proposed single-effect H_2O/LiBr absorption heat pump for combined heating and cooling production. (J. Prieto et al., 2022)

2.2. Air handling unit

The AHU is comprised by a DW, an IEC, a heating coil (HC) and a cooling coil (CC). The AHU can independently control the air temperature (by means of the IEC and the CC), and the air humidity (by means of the DW and HC), thereby optimizing indoor air conditions (Comino et al. 2019). A schematic of the AHU is shown in Figure 3. The DW is activated by means of a heating coil, HC. This HC is fed by a water flow, which is heated by the hot water coming from the AHP condenser and water-solution heat exchanger. The CC is fed by chilled water coming from the AHP evaporator. The process and the regeneration air streams come from the outdoor air (100% outdoor air), as shown in Figure 3.

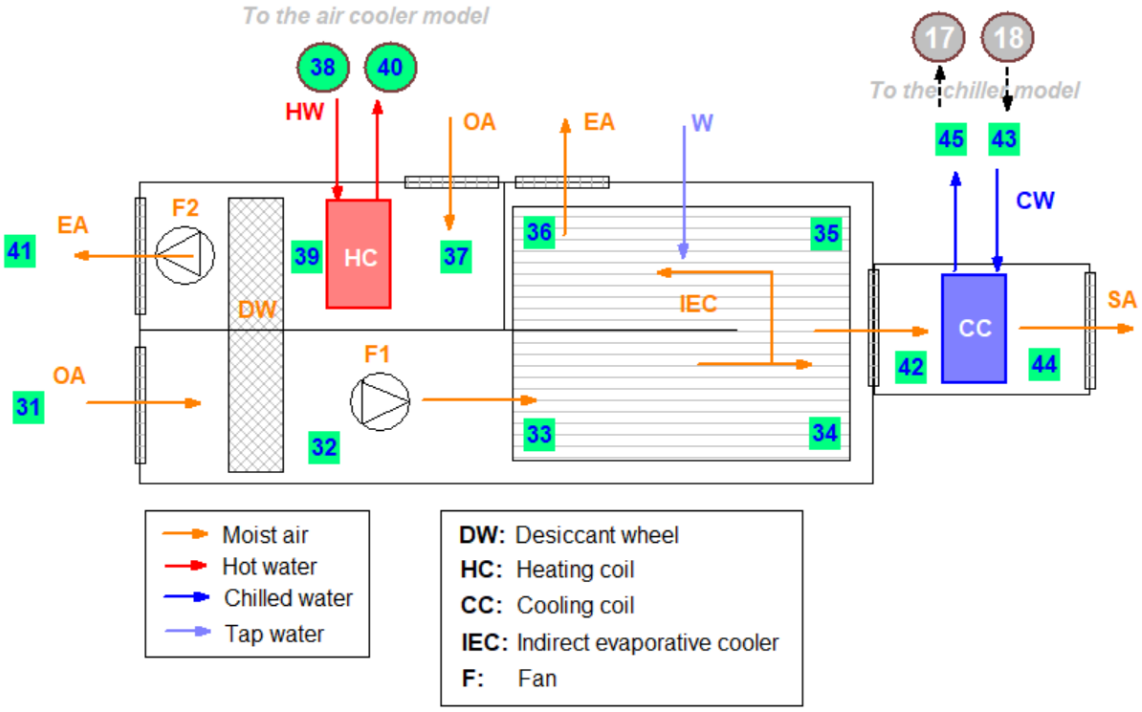

Fig. 3: Air handling unit with desiccant wheel, indirect evaporative cooler, heating coil and cooling coil.

2.3. Solar concentrator thermal collectors

The WeSSun solar concentrator couples flat sun-tracking mirrors to a fixed tilt solar collector (flat plate or evacuated tubular collectors - ETC). It is a low-concentration Design (<2) that, producing a quasi-homogeneous distribution of solar radiation over the solar absorber, increases solar productivity per m^2 of aperture. Moreover, it offers an automatic and simple protection against wind overloads and/or excessive temperatures, by closing the mirrors over the collector, and can be used with existing solar thermal products (see Figure 4 for an example coupling WeSSun with an ETC) (José Ignacio Ajona 2021).

Fig. 4: WeSSun solar concentrator coupling flat sun-tracking mirrors to a fixed tilt evacuated tubular collectors

2.4. Integrated system

The integrated system is a hybrid air conditioning system with the described AHP and the AHU. Figure 5 illustrates how the system is integrated. The AHP is providing chilled water to the cooling coil and hot water to activate the desiccant evaporative cooling system. In this case, chilled water temperature can be increased as the latent heat is handled by the desiccant system. This allows to operate the AHP at higher evaporator temperature.

Therefore, heating rate in the condenser and the water-solution heat exchange is used to activate the desiccant wheel. In this case, hot water passes first through the water-solution heat exchanger and then through the condenser. However, absorber heating rate cannot be used for this application as temperature requirements for the desiccant system are higher than the provided by it. Therefore, absorber heating rate must be dissipated through a cooling tower.

Finally, hot water temperature required for the activation heat is provided by the described solar thermal collectors.

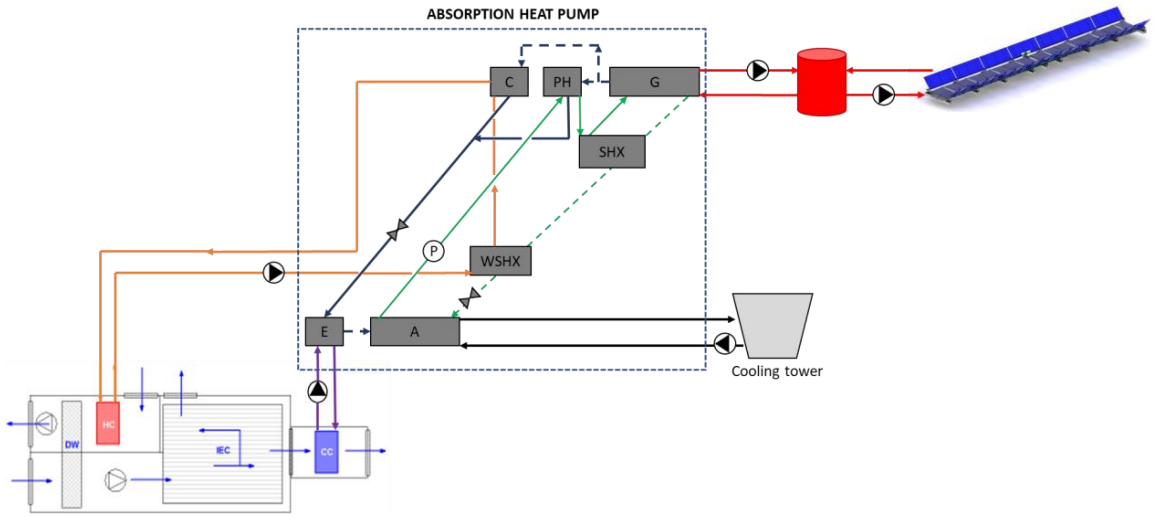

Fig. 5: Overall scheme of the integrated system.

3. Methodology

Models of the single technologies are first developed with Engineering Equation Solver (EES) using the Engineering Equation Solver software package (EES). For the case of the AHP and the AHU, these models are based on energy and mass balances, and heat transfer equations are applied on the thermal components of the system. For the case of the solar thermal collectors, the model is based on the efficiency curve and the incidence angle modifier. Once the models are developed, a performance analysis of the single technologies is firstly done to obtain the optimal working temperatures and flow rates for each one. Then, the technologies are coupled in an integrated model that is used to obtain the component size and nominal conditions that maximizes the system performance in terms of cooling capacity, and overall COP.

3.1. Absorption heat pump model

To model the system properly, typical assumptions for a Water/LiBr absorption cycle are used. The assumptions of the H_2O/LiBr absorption cycle are:

- The absorption cycle operates under equilibrium conditions.
- Losses of heat and pressure decays are neglected.
- Kinetic and potential energies are negligible.
- The water/LiBr solution leaving the absorber is saturated at low pressure.
- The water/LiBr solution leaving the desorber is saturated at high pressure.
- The pure water vapor (refrigerant) leaving the evaporator is saturated at the low pressure.
- Counter-flow desorber is considered, the refrigerant vapor leaving the desorber is in equilibrium with the entering water/LiBr solution.
- Water (refrigerant) at the exit of the condenser is saturated at the high pressure.
- Water (refrigerant) at the exit of the preheater is saturated at the high pressure.
- Preheater and condenser are arranged in parallel, in other words, in both components inlet and outlet conditions are the same.
- The solution pump is isentropic, and the expansion valves are isenthalpic.

Water conditions of the external circuits are calculated with the UA value of each component. Table 1 shows the UA values for all the components of the AHP.

Table 1. UA values for each component of the AHP.

Component	Characteristics	Value	Unit
Evaporator	UA	14.33	kW/C
Condenser	UA	4.734	kW/C
Absorber	UA	27.07	kW/C
Desorber	UA	58.17	kW/C
Preheater	UA	3.00	kW/C
Solution heat exchanger	UA	8.074	kW/C
Water-solution heat exchanger	UA	2.964	kW/C

3.2. Air-handling unit model

To model the system properly, typical assumptions for desiccant systems are used. The assumptions for the AHU are:

- The air-handling unit operates under steady-state conditions.
- Processes occurring in the desiccant wheel are adiabatic.
- There is no mass transfer in the HC, the air humidity ratio ω at the inlet and outlet is constant.
- Cooling process in the IEC occurs at a constant humidity ratio.

The air-handling unit components are modelled by assuming UA value for the heating coil, the thermal effectiveness for the indirect evaporative cooler, the mass effectiveness for the desiccant wheel and the bypass factor for the cooling coil. Table 2 contains the assumed values for each component of the air-handling unit.

Table 2. Specifications of the AHU.

Component	Characteristics	Value	Unit
Heating coil	UA	0.6468	kW/C
Indirect evaporative cooler	ε_t	0.727	-
Desiccant wheel	ε_m	0.52	-
Cooling coil	F	0.2875	-

3.3. Solar thermal collectors

Solar thermal collectors are modelled with the efficiency method, considering that the incidence angle modifier changes with longitudinal and transversal angles. In this sense, the thermal efficiency of the solar collectors is calculated with the following equation:

$$\eta_{SC} = \frac{\dot{Q}_{SC}}{G_0} = a_0 \cdot K(\theta) - a_1 \cdot \frac{(T_{av} - T_{amb})}{G_0} - a_2 \cdot \frac{(T_{av} - T_{amb})^2}{G_0}$$

where $\dot{Q}_{SC}$ is the fluid heating rate in the solar collectors, G_0 is the total solar irradiance, T_{av} is the average temperature of the solar collectors, T_{amb} is the ambient temperature, θ is the incidence angle, a_0, a_1, a_2 are the efficiency parameters, and $K(\theta)$ is the incident angle modifier, which are empirical values provided by the manufacturer. The incident angle modifier is calculated as the product of a transversal (K_T) and a longitudinal (K_L) function:

$$K(\theta) = K_T(\theta_L = 0; \theta_T) \cdot K_L(\theta_L; \theta_T = 0)$$

Figure 6 shows the transversal and the longitudinal incidence angle modifiers as function of the incidence angle.

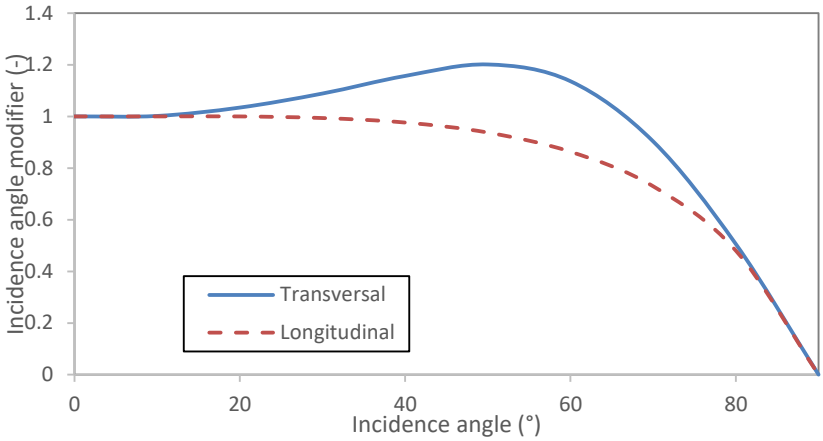

Fig. 6: Solar thermal collector longitudinal and transversal incidence modifiers.

The technical characteristics of the solar thermal collectors are included in Table .

Table 3. Technical characteristics of the solar thermal collectors.

Parameter	Value	Description
Dimensions (mm)	1420, 2050, 100	Length, width, height
Aperture area (m^2)	4.46	-
Number of vaacuum tubes (-)	21	-
Concentration ratio (-)	1.704	-
a_0 (-)	0.642	Based on aperture area
$a_1 \left(\frac{W}{m^2 \cdot K}\right)$	0.89	Based on aperture area
$a_2 \left(\frac{W}{m^2 \cdot K^2}\right)$	0.001	Based on aperture area
Volume Flow rate (l/h)	10-500	-
Max. operating pressure (bar)	10	-
Stagnation temperature (ºC)	272	-
Mirror solar reflectivity	> 94 %	-
Mirror dimensions (mm)	1495, 1605, 4	Length, width, heigth

The total number of solar thermal collectors is 20 and the water tank volume is 9.0 m^3.

4. Results

Results section is divided into two subsections. The first subsection is focus on the performance evaluation of the AHP. The second subsections is focus on the performance evaluation of the integrated system.

4.1. Performance evaluation of the AHP

Figure 7 shows the AHP Cooling coefficient of performance (COP_C) and heating coefficient of performance (COP_H) as function of the outlet condenser temperature, the chilled water temperature, the ambient temperature and the activation temperature. In terms of COP_C, values follow the typical trend of the single-effect absorption chillers, but with higher values (from 0.82 to 0.93) due to the lower heat input required in the generator. The COP_H is especially influenced by the driving hot water inlet temperature, with stable values (0.87–0.93).

The summary of the trends for the COP_C and the COP_H is included in Table 4. In general, the higher the condenser and the chilled water temperatures, the higher the COP_C and COP_H. On the other hand, the higher the ambient temperature, the lower the COP_C and COP_H. The activation temperature has an opposite effect on the COP_C and the COP_H. In this sense, the higher the activation temperature, the higher the COP_C and the lower the COP_H.

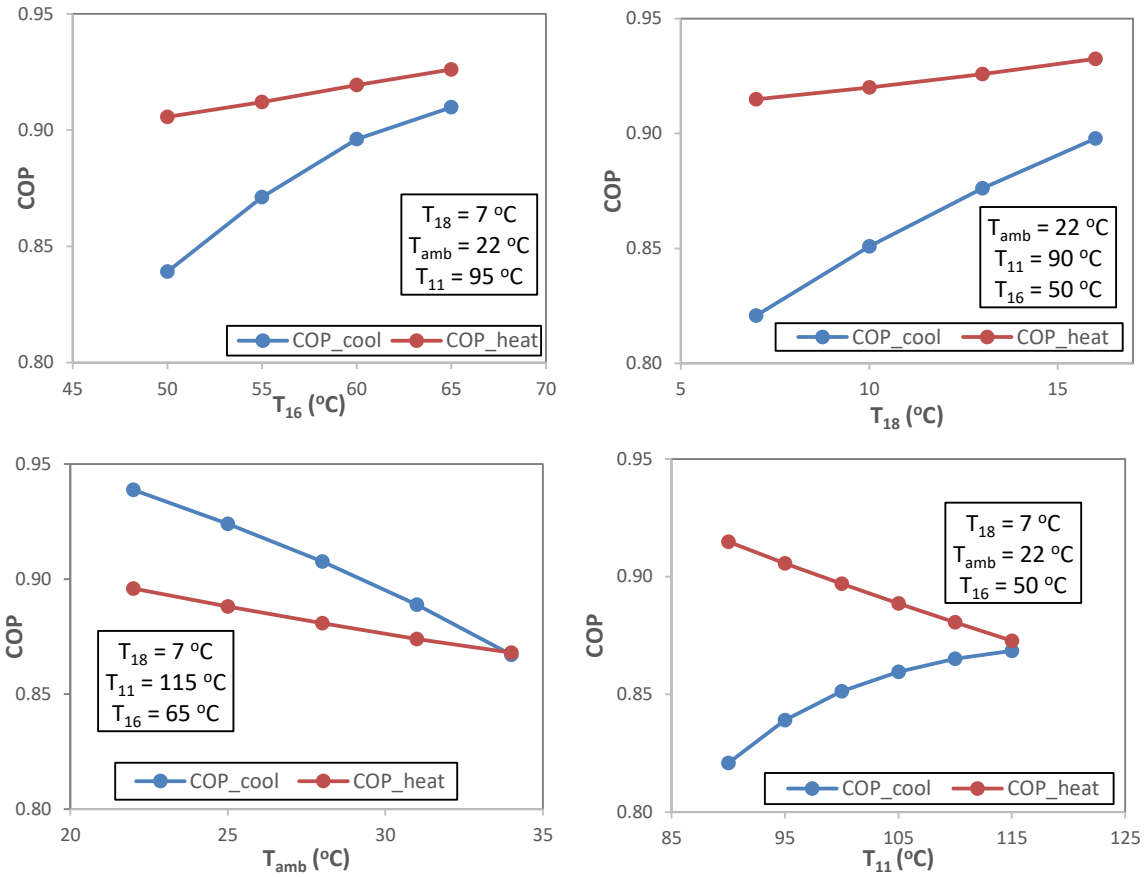

Fig. 7: AHP Cooling COP and heating COP as function of the outlet condenser temperature (top-left), the chilled water temperature (top-right), the ambient temperature (bottom-left) and the activation temperature (bottom-right).

Table 2. Results of the mathematical modelling of the AHP.

Indicator	Trend	COP_{cool} Trend	COP_{heat} Trend
T_{16}	increase ↑	increase ↑	increase ↑
T_{18}	increase ↑	increase ↑	increase ↑
T_{amb}	increase ↑	decrease ↓	decrease ↓
T_{11}	increase ↑	increase ↑	decrease ↓

4.2. Performance evaluation of the integrated system

Once the performance of the AHP is evaluated, the performance of the integrated system is carried out. Table 5 shows the input parameters considered for the simulation of the integrated system. Ambient temperature ranges from 22 °C to 34 °C. Ambient relative humidity ranges from 0.4 to 0.8. Chilled water temperature ranges from 7 °C to 10 °C, outlet condenser temperature ranges from 60 °C to 65 °C and activation temperature ranges from 100 °C to 105 °C. In total, 120 operational conditions are evaluated from the integrated system.

The performance of the integrated system is evaluated in terms of total cooling ($Q_{cool,tot}$), which is calculated as the total cooling production of the system (the provided by the IEC and the CC); total COP (COP_{tot}), which is calculated as the $Q_{cool,tot}$ over the activation heat required in the AHP.

Table 5. The updated list of input parameters for the simulation of the integrated system.

RH_{amb}	T_{amb} ºC	T_{18} ºC	T_{16} ºC	T_{11} ºC
0.4	22	7	60	100
0.6	25	10	65	105
0.8	28			
	31			
	34			

The main results of the simulations are included in Table 6. This Table shows the highest COP_{tot} and $Q_{cool,tot}$ achieved by the integrated system under different ambient conditions, and the operational conditions that allow to achieving this performance. Generally, the highest COP_{tot} is achieved at T_{16}=65 ºC and T_{11}=100 ºC. On the other hand, the highest $Q_{cool,tot}$ is achieved at T_{18}=10 ºC, T_{16}=60 ºC, and T_{11}=105 ºC.

Table 6. Operating conditions at RH_{amb} = 0.6 and different ambient temperatures T_{amb} = 22 - 34 ºC.

T_{11} = 105 ºC		COP_{tot}	$Q_{cool,tot}$	T_{18} ºC	T_{16} ºC	T_{11} ºC
T_{amb}=22 ºC	Highest COP_{tot}	1.113		7	65	100
RH_{amb}=0.6	Highest $Q_{cool,tot}$		84.35	10	60	105
T_{amb}=25 ºC	Highest COP_{tot}	1.143		7	65	100
RH_{amb}=0.6	Highest $Q_{cool,tot}$		76.60	10	60	105
T_{amb}=28 ºC	Highest COP_{tot}	1.16		7	65	100
RH_{amb}=0.6	Highest $Q_{cool,tot}$		68.93	10	60	105
T_{amb}=31 ºC	Highest COP_{tot}	1.209		10	65	100
RH_{amb}=0.6	Highest $Q_{cool,tot}$		61.33	10	60	105
T_{amb}=34 ºC	Highest COP_{tot}	1.192		10	65	100
RH_{amb}=0.6	Highest $Q_{cool,tot}$		53.79	10	60	105

5. Conclusions

This study presents an energy analysis and performance evaluation of an integrated solar-driven air conditioning system using an AHP with condensation heat recovery and an AHU with a DW and IEC. The AHP is activated with ETC with mirrors with low concentration design (<2). The single components of the system and the integrated system have been numerically evaluated.

First, the performance of the AHP is separately evaluated. The results for the AHP simulations are presented in Figure 7 and Table 4. In general, the higher the condenser and the chilled water temperatures, the higher the COP_C and COP_H. On the other hand, the higher the ambient temperature, the lower the COP_C and COP_H. The activation temperature has an opposite effect on the COP_C and the COP_H. In this sense, the higher the activation temperature, the higher the COP_C and the lower the COP_H.

The, the integrated system is studied. In this case, the highest COP_{tot} achieved by the system is 1.21, which is reached with an ambient temperature of 31 ºC, a chilled water temperature of 10 ºC, an outlet condenser temperature of 65 ºC and an activation temperature of 100 ºC. The highest cooling capacity achieved by the system is 84.35 kW, which is reached with an ambient temperature of 22 ºC, a chilled water temperature of 10 ºC, an outlet condenser temperature of 60 ºC and an activation temperature of 105 ºC.

6. Acknowledgments

This work has been supported by the European WEDISTRICT project (grant agreement N°857801) co-founded by the EC under the call H2020-LC-SC3-2018-2019-2020.

7. References

Ajona, J.I, 2021. Advanced Tracking Concentrator for Fixed Tilt solar thermal Collectors. European Federation of Agencies and Regions for Energy and Environment (FEDARENE)

Prieto, J., Ayou, D.S., Coronas, A. 2022. Energy and Exergy Analysis of H_2O/LiBr Absorption Heat Pumps for Combined Heating and Cooling Applications. CYTEF 2022 − XI Congreso Ibérico | IX Congreso Iberoamericano de Ciencias y Técnicas del Frío, Cartagena, Spain, 17-19 April, 2022.

Comino, F., Castillo, J., Navas, F.J., Ruiz de Adana, M.. Experimental assessment of a hybrid solar HVAC system based on desiccant wheel and an indirect evaporative cooling. Preliminary experimental results. Conference: II International Engineering Thermodynamics Congress, Albacete, Spain, June, 2019